Eur. Phys. J. A **14**, 159–167 (2002)
DOI 10.1140/epja/i2001-10201-5

**THE EUROPEAN PHYSICAL JOURNAL A**



# High-spin states in $^{36}$Ar and their underlying shell model configurations

H. Röpke[a], J. Brenneisen, and M. Lickert

Fakultät für Physik der Universität Freiburg, Freiburg i.Br., Germany

Received 21 December 2001
Communicated by D. Schwalm

**Abstract.** Eight high-spin states in $^{36}$Ar below 10 MeV excitation energy, among them a prospective $J^\pi = 8^-$ state at 9408 keV and the $J \leq 8$ levels of the recently discovered superdeformed rotational band, have been observed by n-$\gamma$ coincidence measurements with the $^{33}$S$(\alpha, \mathrm{n}\gamma)$ reaction at $E_\alpha = 14.4$ and 13.4 MeV. High-spin assignments of, respectively, $J^\pi = 6^+$ and $5^-$ were obtained for the $E_\mathrm{p} = 1209$ and 1462 keV ($E_x = 9682$ and 9927 keV) resonances of the $^{35}$Cl$(\mathrm{p}, \gamma)$ reaction by a measurement of $\gamma$-ray angular distributions. The spectrum of the high-spin and of the $E_x \leq 7.4$ MeV levels is decomposed according to the underlying shell model configurations with $n = 0, 1, 2, 4$ particles excited from the $N = 2$ into the $N = 3$ major shell. The role of four-particle excitations, all connected with large prolate distortions, is elucidated for the entire $A = 36$–40 mass region.

**PACS.** 27.30.+t $20 \leq A \leq 38$ – 21.60.Cs Shell model – 21.10.Re Collective levels

## 1 Introduction

Nuclei in the vicinity of shell gaps are still a challenge to nuclear-structure calculations because of low-lying multi-particle excitations across the gap. Excitations across the gap between the $N = 2$ and $N = 3$ major shells of the harmonic oscillator (the *s*-*d* and *f*-*p* shells) have been studied for a variety of nuclei near the closure of the *s*-*d* shell in $^{40}$Ca. The role of two-particle excitations has been elucidated for $^{35\text{-}37}$Cl [1] $^{37,39}$Ar [1–3] $^{38,39}$K [4,5] by studies of their high-spin states. In the case of $^{38}$Ar [6] and $^{40}$Ca [7] four-particle excitations which are connected with strong deformation [8] occur below the two-particle excitations and lead to the phenomenon of shape coexistence. The complete set of *n*-particle excitations with $n = 1$–4 could be studied in the case of $^{38}$Ar [9]. An important piece of information which was still missing at the beginning of this work was the structure of the $A = 36$, $T = 0$ states which occur in $^{36}$Ar only. The prospects for disentangling the various contributions to the level scheme are good because the "trivial" but most numerous part is well under control theoretically. The levels of pure *s*-*d* origin (dubbed the $0\,\hbar\omega$ excitations) are reliably predicted, to an accuracy of 100–200 keV, by shell model calculations in the unrestricted *s*-*d* basis space using the universal *s*-*d* shell (USD) interaction of Wildenthal [10]. The spectrum of states which arise from the promotion of one particle into the *f*-*p* shell ($1\,\hbar\omega$ excitations) has been calculated, to an accuracy of roughly 500 keV, by Warburton *et al.* [11] using the USD interaction for *s*-*d* nucleons, the McGrory interaction [12] for *f*-*p* nucleons and the WMBM cross-shell interaction developed by the authors. The $T = 0$ spectrum of $^{36}$Ar shows [13] a total of 28 levels up to 7.4 MeV excitation energy, six of which remain unaccounted for if only $0\,\hbar\omega$ and $1\,\hbar\omega$ excitations are considered. Experience shows that the situation could be clarified if the spectrum of high-spin states in $^{36}$Ar were known as it is the case in the neighbouring nuclei. The highest assigned spin at the beginning of this work was, however, $J = 4$ only in connection with positive parity and $J = 6$ in connection with negative parity [13]. The present work has tried to provide the missing experimental information by the combined studies of the $^{33}$S$(\alpha, \mathrm{n}\gamma)$ and $^{35}$Cl$(\mathrm{p}, \gamma)$ reactions. The combination of ($\alpha$,n$\gamma$) and (p,$\gamma$) reactions has proved successful in the comparable cases of the $A = 4$n nuclei $^{32}$S [14] and $^{28}$Si [15,16]. Concurrent work with the $^{24}$Mg ($^{20}$Ne, $2\alpha$) reaction [17] emphasises a special type of states, members of a $K^\pi = 0^+$ rotational band in analogy to the known bands in $^{38}$Ar [6] and $^{40}$Ar [18]. The $^{36}$Ar band was traced up to $J^\pi = 16^+$ and $E_x = 22.364$ MeV. The present work will yield a more complete accounting of the high-spin states in $^{36}$Ar but is confined, on the other hand, to $E_x < 10$ MeV and $J \leq 8$.

[a] e-mail: muehelga@uni-freiburg.de

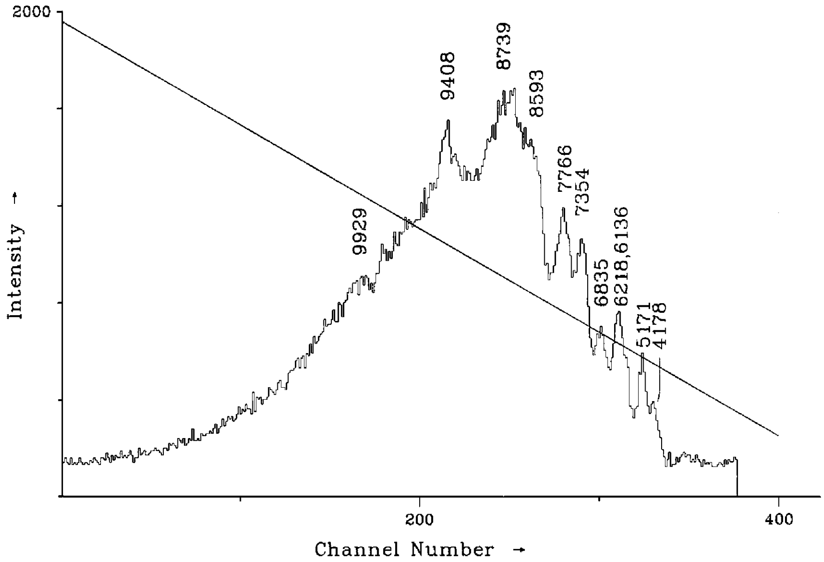


**Fig. 1.** Neutron-TOF spectrum from the $^{33}$S($\alpha$, n$\gamma$) reaction at $E_\alpha = 14.4$ MeV in coincidence with $\gamma$-rays detected in the plastic scintillator. Labels on the neutron groups give the corresponding excitation energies (keV) of levels in the residual nuclide $^{36}$Ar. The TOF can be obtained with the aid of the straight calibration line by TOF (ns) = 0.1 × Intensity.

## 2 Experimental procedure

### 2.1 Measurements with the $^{33}$S($\alpha$, n$\gamma$) reaction

A target of 240 $\mu$g/cm$^2$ CdS, isotopically enriched in $^{33}$S to 48%, and evaporated onto a tantalum backing was bombarded with a 40 nA $\alpha$-particle beam from the 7 MV Van de Graaff accelerator of the University of Freiburg. The beam energies were 14.4 and 13.4 MeV. Coincidences between neutrons and $\gamma$-rays were recorded using a neutron time-of-flight (TOF) spectrometer and, simultaneously, a 120 cm$^3$ Ge(Li) detector and a 7.5 cm diameter × 7.5 cm thick plastic scintillator for the detection of $\gamma$-rays. The TOF spectrometer, which has been described previously [15], consists of 19 liquid-scintillation detectors in a quasi-annular array placed at zero degrees with respect to the beam at a distance of 2 m from the target. Each detector has its own n-$\gamma$ pulse shape discrimination [19]. The start pulse of the TOF spectrometer was provided by neutron events, the stop pulse by $\gamma$-events in either of the two $\gamma$-ray detectors. For every coincident event, the information on neutron time-of-flight and $\gamma$-ray pulse height was stored on a magnetic tape. The time resolution of the spectrometer was 2 ns in combination with the plastic scintillator and 6 ns in combination with the Ge(Li) detector. Both $\gamma$-ray detectors were placed at 135 degrees with respect to the beam where angular correlations have a negligible influence on the observed $\gamma$-ray intensities because of a vanishing value of the second Legendre polynomial.

### 2.2 The $^{35}$Cl(p, $\gamma$) measurements

Measurements of $\gamma$-ray angular distributions were performed on selected resonances of the $^{35}$Cl(p, $\gamma$) reaction. Targets of 30 $\mu$g/cm$^2$ $BaCl_2$, isotopically enriched in $^{35}$Cl to 80% and evaporated onto a tantalum backing were bombarded by a 4 $\mu$A proton beam. Though direct water cooling of the targets was employed, it was difficult to perform extended runs of more than 24 hours duration with a single target only. Gamma-ray singles spectra were recorded with two 120 cm$^3$ high-purity germanium detectors of 2 keV resolution at the $^{60}$Co energies. One of the detectors which served as the monitor was placed at 55 degrees with respect to the beam, while the other detector was placed consecutively at angles of 0, 30, 45, 60 and 75 degrees. The run time was typically 12 hours per angle. The distance between the detector front face and the target was 4 cm.

## 3 Results

### 3.1 Results obtained with the $^{33}$S($\alpha$, n$\gamma$) reaction

The bombarding energies of 14.4 and 13.4 MeV were chosen to facilitate the investigation of $^{36}$Ar levels in the badly explored region above 7.4 MeV excitation energy. The kinematics of the reaction combined with the detection threshold for neutrons, which is roughly 1 MeV, allows the investigation of levels up to 10.5 MeV excitation energy. The levels above $E_x = 8.51$ MeV are already unstable to proton decay [13]. The selectivity of the ($\alpha$,n) reaction, which favours the population of high-spin states, is thus enhanced by the competition between the proton and the $\gamma$-decay of the levels. The $\gamma$-decaying states have high spin ($J \geq 6$ in general) so that their proton decay is effectively suppressed by the centrifugal barrier. The slow-neutron groups of fig. 1 are consequently due to one or two levels only in spite of level densities of the order of 50/MeV. The degradation of resolution by use of the Ge(Li) detector instead of the plastic scintillator is thus

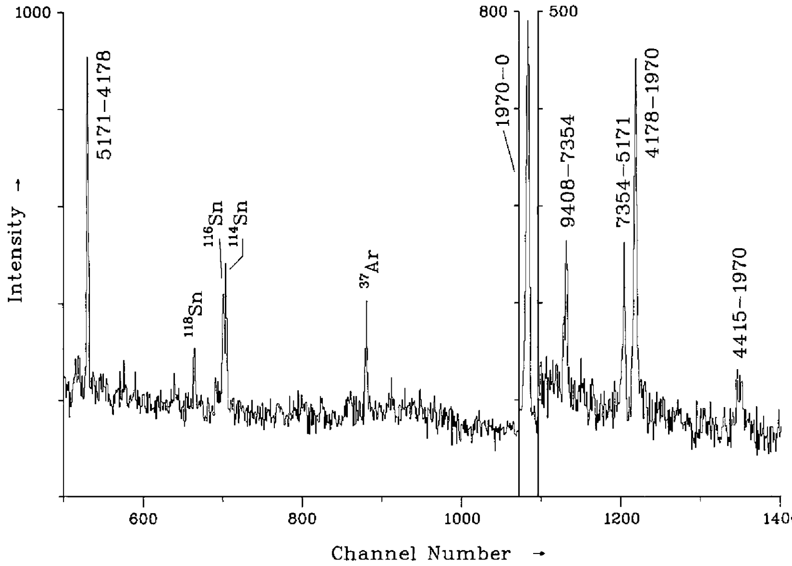


**Fig. 2.** Gamma-ray spectrum from the $^{33}$S$(\alpha, \mathrm{n}\gamma)$ reaction at $E_\alpha = 14.4$ MeV taken in coincidence with neutrons leading to a new high-spin state at $E_x = 9408$ keV. Gamma-decay to the 7354 keV, $J^\pi = 6^-$ yrast state is visible as it is the subsequent decay. Contaminant $\gamma$-rays are labelled with the symbol of the nuclide from which they arise.

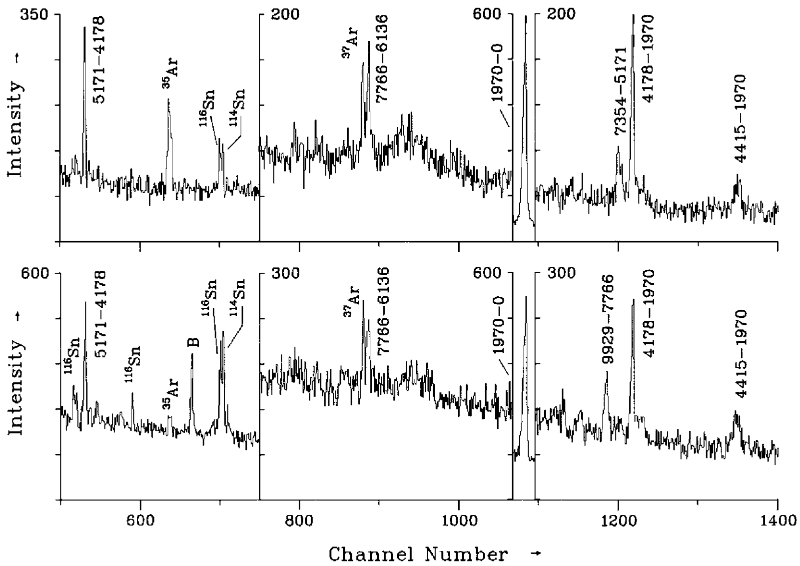


**Fig. 3.** Same as fig. 2. The upper/lower spectra are taken in coincidence with neutrons leading to the 7766/9929 keV levels which have been identified in a concurrent work [17] as the $J^\pi = 6^+/8^+$ members of a superdeformed $K^\pi = 0^+$ rotational band. The existence of a $9929 \to 7766 \to 6136$ keV cascade of inband decays is clearly visible. The symbol B stands for an unidentified background radiation of 1230 keV energy.

not a menace. The more serious problem is the overload of the $\gamma$-ray detector by the prolific $^{32}$S$(\alpha, \mathrm{p}\gamma)$ reaction, which delimits the useful $\gamma$-ray counting rate. Gamma-ray spectra were generated from the n-$\gamma$ coincidence matrix by setting 10 ns wide windows in the TOF spectra. Examples which employ somewhat broader windows for the sake of statistical accuracy are given in figs. 2, 3. The systematic analysis of $\gamma$-ray spectra yielded the decay modes of eight levels (table 1) which were unknown at the beginning of this work. The 7766, 9186 and 9929 keV levels are, however, present in a concurrent investigation [17] of the $^{24}$Mg$(^{20}$Ne$, 2\alpha)^{36}$Ar reaction. The reported $\gamma$-decay of the 9929 keV level is in agreement with the present work. The 7766 keV level shows a second, weaker-decay mode to the 4415 keV, $J^\pi = 4^+$ level which cannot be claimed with safety from the present work. The 9186 keV level of [17] has a single-decay mode to the 4415 keV, $J^\pi = 4^+$ state only while we observe a second mode leading to the 5171 keV, $J^\pi = 5^-$ state.

All levels have safe $T = 0$ assignments since the spectrum of $T = 1$ states at these energies is already known (table 36.22 of [13]). The observed $\gamma$-decays of the new lev-

**Table 1.** Energies and $\gamma$-decay modes of high-spin, $T = 0$ states in $^{36}$Ar between 7.4 and 10 MeV excitation energy.

| Levels from the $^{33}$S($\alpha$, n$\gamma$) reaction | | | | | Levels from the $^{35}$Cl(p, $\gamma$) reaction$^{a)}$ | | | | | Shell model | |
|---|---|---|---|---|---|---|---|---|---|---|---|
| Level | | Decay to | | Branch (%) | Level | | Decay to | | Branch (%) | | |
| $E_i$ (MeV) | $J^{\pi\,b)}$ | $E_f$ (MeV) | $J^\pi$ | | $E_i$ (MeV) | $J^{\pi\,b)}$ | $E_f$ (MeV) | $J^\pi$ | | $E_x$ (MeV) | $J^\pi$ |
| 7.766 ± 4 | $6^{+\,c)}$ | 6.136 | | | 9.682 | $6^+$ | 4.415 | $4_1{}^+$ | 100 | 8.286 | $5_3{}^{-\,e)}$ |
| 8.288 ± 4 | $\pi = -$ | 5.896 | $4_2{}^-$ | | 9.764 | $\pi = -$ | 4.178 | $3_1{}^-$ | 8 | 8.578 | $7_1{}^{-\,e)}$ |
| 8.593 ± 4 | $\pi = -$ | 6.217 | $5_2{}^-$ | | | | 4.415 | $4_1{}^+$ | 35 | 8.657 | $5_4{}^{-\,e)}$ |
| 8.739 ± 4 | $\pi = -$ | 5.171 | $5_1{}^-$ | | | | 5.171 | $5_1{}^-$ | 37 | 9.1 | $6_1{}^{+\,g)}$ |
| 8.919 ± 4 | $\pi = -$ | 5.171 | $5_1{}^-$ | | | | 5.857 | $3_2{}^-$ | 4 | 9.2 | $6_2{}^{+\,f)}$ |
| 9.186 ± 4 | | 5.171 | $5_1{}^-$ | 50 ± 10 | | | 6.837 | $3_3{}^-$ | 18 | 9.038 | $6_2{}^{-\,e)}$ |
| | | 4.415 | $4_1{}^+$ | 50 ± 10 | 9.927 | $5^-$ | 4.415 | $4_1{}^+$ | 62 | 9.056 | $5_5{}^{-\,e)}$ |
| 9.408 ± 4 | $(8^-)$ | 7.354 | $6_1{}^-$ | | | | 5.171 | $5_1{}^-$ | 9 | 9.379 | $7_2{}^{-\,e)}$ |
| 9.929 ± 4 | $8^{+\,c)}$ | 7.766 | | | | | 5.857 | $3_2{}^-$ | 10 | 9.411 | $5_6{}^{-\,e)}$ |
| | | | | | | | 6.136 | | 3 | 9.474 | $6_3{}^{-\,e)}$ |
| | | | | | | | 6.217 | $5_2{}^-$ | 1 | 9.696 | $6_3{}^{+\,d)}$ |
| | | | | | | | 6.837 | $3_3{}^-$ | 6 | 9.730 | $5_7{}^{-\,e)}$ |
| | | | | | | | 7.259 | $3_4{}^-$ | 5 | 10.783 | $8_1{}^{-\,e)}$ |
| | | | | | | | | | | 11.2 | $8_1{}^{+\,g)}$ |

a) Ref. [21].
b) From the present work if not otherwise stated.
c) Ref. [17].
d) $0\,\hbar\omega$ state from [10].
e) $1\,\hbar\omega$ state from [11].
f) $2\,\hbar\omega$ state read, with 100 keV uncertainty, from fig. 3 of [17].
g) $4\,\hbar\omega$ state read, with 100 keV uncertainty, from fig. 3 of [17].

els are thus of isoscalar nature and subject to the strong hindrance in the $E1$ sector [20]. Hence we feel safe to assign negative parity to those states which decay exclusively to negative-parity levels. By the same token equal parity can be inferred for the levels at 6136, 7766 and 9929 keV excitation energy. We are able in the following subsection to assign $J^\pi = 4^+$ to the 6136 keV level but meanwhile assignments of, respectively, $J^\pi = 4^+$, $6^+$ and $8^+$ exist for all three levels [17]. The 9408 keV level with its exclusive decay to the $6^-$ yrast state receives a tentative $J^\pi = 8^-$ assignment which will be backed up later by the results of a shell model calculation.

### 3.2 Results obtained with the $^{35}$Cl(p, $\gamma$) reaction

Table 1 includes the small number of $^{35}$Cl(p, $\gamma$) resonances from [21] which, on the basis of their cited $\gamma$-decay modes, are candidates of high-spin ($J \geq 5$) assignments. They are complementary to the high-spin states of the $^{33}$S($\alpha$, n$\gamma$) reaction which have $\Gamma_p < \Gamma_\gamma$, while the resonances have proton width comparable to or larger than the widths for the $\gamma$-decay. The $E_x = 9927$ keV, $E_p = 1462$ keV resonance offers the possibility of obtaining a spin-parity assignment to the important 6136 keV level. (A warning: This resonance must not be confused with the 9929 keV level from the $^{33}$S($\alpha$, n$\gamma$) reaction which is also seen in the $^{24}$Mg($^{20}$Ne, 2$\alpha$) reaction at 9927 keV.) The $E_x = 9682$ keV, $E_p = 1209$ keV resonance with its exclusive decay to the 4415 keV, $4^+$ state could correspond to the sole high-spin state in the $0\,\hbar\omega$ spectrum below 10 MeV, a $J^\pi = 6^+$ state predicted to occur at 9696 keV [10]. Both resonances have $T = 0$ assignments because the spectrum of $T = 1$ states at these energies is already complete (table 36.22 of [13]). The observed $\gamma$-decays to $T = 0$ states are of the isoscalar type and inherently weak in the case of dipole and magnetic quadrupole transitions. This is reflected by small values of the resonance strengths $S = (2J+1)\Gamma_p\Gamma_\gamma/\Gamma$ which amount to 300 meV for the $E_x = 9927$ keV and to 120 meV for the 9682 keV state [13]. By applying the recommended upper limits of multipole transition rates [20] spin-parity assignments of $J^\pi = 3^-$, 4, $5^-$ can be made in the former case and $J^\pi = 2^+$, 3–5, $6^+$ in the latter one. The final assignments to both resonances and the interesting 6136 keV level as well follow from the measurement and analysis of the angular distributions (relative to the beam axis) of primary and secondary $\gamma$-radiations. Table 2 gives the results of the measurements in terms of the coefficients $A_2$ and $A_4$ of a Legendre-polynomial expansion

$$W(\theta) = N\big(1 + Q_2A_2P_2(\cos\theta) + Q_4A_4P_4(\cos\theta)\big), \quad (1)$$

with $N$ being the overall normalization and $Q_2, Q_4$ attenuation coefficients which take into account the averaging of $P_2(\cos\theta)$ and $P_4(\cos\theta)$ due to the finite solid angle of the $\gamma$-ray detector. We use the values $Q_2 = 0.87$, $Q_4 = 0.6$. The angular distributions have been analyzed

**Table 2.** Results of $\gamma$-ray angular distribution measurements on resonances of the $^{35}$Cl(p, $\gamma$) reaction.

| Transition | | | | Angular distribution coefficients | | | | Quadrupole/dipole mixing ratio $\delta$ |
|---|---|---|---|---|---|---|---|---|
| | | | | Exp. | | Theor. | | |
| $E_\mathrm{i}$ (keV) | $J_\mathrm{i}^{\pi\,\mathrm{a)}}$ | $E_\mathrm{f}$ (keV) | $J_\mathrm{f}^{\pi\,\mathrm{a)}}$ | $A_2$ | $A_4$ | $A_2$ | $A_4$ | |
| 9927 | $\underline{5}^-$ | 4415 | $4^+$ | $-0.33 \pm 0.04$ | $0.027 \pm 0.05$ | $-0.32$ | 0.00 | $0.02 \pm 0.05$ |
| 4415 | $4^+$ | 1970 | $2^+$ | $0.40 \pm 0.02$ | $-0.18 \pm 0.03$ | 0.41 | $-0.17$ | $\infty$ |
| 9927 | $5^-$ | 5857 | $3^-$ | $0.42 \pm 0.07$ | $-0.44 \pm 0.10$ | 0.41 | $-0.17$ | $\infty$ |
| 9927 | $5^-$ | 6136 | $\underline{4}^+$ | $-0.17 \pm 0.05$ | $0.05 \pm 0.05$ | $-0.17$ | 0.00 | $-0.06 \pm 0.03$ |
| 9682 | $\underline{6}^+$ | 4415 | $4^+$ | $0.39 \pm 0.05$ | $-0.19 \pm 0.07$ | 0.41 | $-0.17$ | $\infty$ |
| | $\underline{4}^+$ | | | | | 0.38 | $-0.16$ | $-1.1 \pm 0.4$ |
| 4415 | $4^+$ | 1970 | $2^+$ | $0.33 \pm 0.03$ | $-0.18 \pm 0.04$ | 0.41 | $-0.17$ | $\infty$ |
| | | | | | | $0.30^{\mathrm{b)}}$ | $-0.03^{\mathrm{b)}}$ | |

a) The underlined $J^\pi$ assignments are results of the present work, all others are adapted from [13].
b) Alternative coefficients obtained for $J^\pi(9682) = 4^+$.

by considering dipole and quadrupole contributions to the $\gamma$-radiations and proton capture with orbital angular momentum $\ell \leq 4$. Capture with $\ell = 4$ was, however, neglected if $\ell = 2$ was possible. For justification see [22]. The channel-spin quantum number can adopt values $s = 1, 2$. The theoretical expressions for $W(\theta)$ in the frame of the channel-spin representation are given by (3.42) and (3.58) of Rose and Brink [23]. The angular distributions of primary and secondary $\gamma$-decays, as they are given in table 2, were analyzed simultaneously. The value of secondary transitions of the stretched quadrupole type ($J \to J-2$ transitions) as they occur for both resonances, has been discussed in [22]. In the present cases they indicate good alignment of the resonance spin ($J$ perpendicular to the beam axis) which happens if the quantum numbers of orbital angular momentum and of channel spin just add up to the quantum number of the resonance spin. The detailed $\chi^2$-fits yield in fact the formation of the $E_x = 9927$ keV resonance with $\ell = 3$, $s = 2$ resulting in a $J^\pi = 5^-$ assignment to this state. The 6136 keV level fed on this resonance receives a $J^\pi = 4^+$ assignment knowing [13] that its parity is natural. In the case of the $E_x = 9682$ keV resonance, the alternatives $\ell = 4$, $s = 2$, $J^\pi = 6^+$; $\ell = 2$, $s = 2$, $J^\pi = 4^+$; $\ell = 3$, $s = 1$, $J^\pi = 4^-$ remain with the last possibility being excluded because of an unacceptably large ($> 10$ W.u.) $M2$ rate for the $9682 \to 4415$ keV transition. The quadrupole/dipole mixing ratio adopts a value around $\delta = -1.1$, almost identical with the result obtained for the $J^\pi = 4^+$ alternative (table 2). Such values are characteristic of a famous ambiguity in the analysis of $\gamma$-ray angular distributions. A stretched quadrupole transition (spin sequence $J \to J-2$) can always be simulated [24] by a $J \to J$ transition with a mixing ratio $\delta \sim -1.2$. Hence we consider the $J^\pi = 4^+$ alternative as rather formal, especially since the $J^\pi = 6^+$ alternative fulfills a stringent requirement. The $A_2$ and $A_4$ coefficients of the primary $9682 \to 4415$ keV, $6^+ \to 4^+$ and of the secondary $4415 \to 1970$ keV, $4^+ \to 2^+$ transitions must be identical. The quantities $W_\mathrm{p}(\theta)N_\mathrm{s}/W_\mathrm{s}(\theta)N_\mathrm{p}$ explained by eq. (1) must have a value of one independent of the angle. The uncertainties of the monitor have cancelled in this expression and the errors of the norms are negligible. We observe pure scatter around a value of 1.01 with a maximum deviation of 0.03.

The 9764 keV resonance was not investigated here but the low-energy transitions to negative-parity states, all of isoscalar character, are strongly indicative of negative parity.

### 3.3 Reassessment of older data

Before we enter a discussion of the $^{36}$Ar level scheme it is necessary to remove an erroneous interpretation of some old data in the compilation of [13]. The very early investigation of the $^{36}$Ar level scheme with the $^{39}$K(p, $\alpha$) reaction [25] had yielded a level at $E_x = 6.66 \pm 0.02$ MeV. An improved calibration of the $\alpha$-particle spectrum using today's precise $^{36}$Ar energies leads to $E_x = 6632$ keV and a reduction of the uncertainty to less than 10 keV. Up to now it was believed that the level in question had been observed [21] in the $\gamma$-decay of the $^{35}$Cl(p, $\gamma$) resonance with $E_x = 10220$ keV, $J, T = 4, (1)$ leading to an assignment $J^\pi = 2$–$4^+$. A cascade of two $\gamma$-rays with energies of, respectively, 3574 and 2205 keV was believed to connect the resonance with the 4440 keV, $J^\pi = 2^+$ state via an intermediate state at 6645 keV. In view of the keV accuracy of $\gamma$-ray energies in radiative capture work it is impossible to interpret the established 6632 keV level as the intermediate state. Turning the $\gamma$-ray cascade upside down leads to a hitherto unobserved intermediate state at 8015 keV, not to be confused with the 8016 keV, $J^\pi = 4^-$ level of [21], and leaves the $J^\pi$ assignment to the known 6632 keV state completely open. The feeding of the new 8015 keV level must proceed by isovector dipole radiation in view of the large strength $(2J+1)\Gamma_\mathrm{p}\Gamma_\gamma/\Gamma = 2.9$ eV of the feeding 10220 keV resonance, thus delimiting its quantum numbers to $J, T = 3$–$5, 0$. The new results make sense under the (most natural) assumption that the feeding resonance and the new level belong to the $0\,\hbar\omega$ shell model config-

**Table 3.** The $E_x < 7.4\,\mathrm{MeV}$, $T = 0$ states of $^{36}$Ar.

| Exp. level[a)] | | Model states | | | | | | | |
|---|---|---|---|---|---|---|---|---|---|
| | | $0\,\hbar\omega$[e)] | | $1\,\hbar\omega$[f)] | | $4\,\hbar\omega$[g)] | | $2\,\hbar\omega$[h)] | |
| $E_x$ (MeV) | $J^\pi$ | $E_x$ (MeV) | $J^\pi$ | $E_x$ (MeV) | $J^\pi$ | $E_x$ (MeV) | $J^\pi$ | $E_x$ (MeV) | $J^\pi$ |
| 0. | $0^+$ | 0. | ${0_1}^+$ | | | | | | |
| 1.970 | $2^+$ | 1.927 | ${2_1}^+$ | | | | | | |
| 4.178 | $3^-$ | | | 5.049 | ${3_1}^-$ | | | | |
| 4.329 | $(0–2)^+$ | | | | | 5.6 | $0^+$ | | |
| 4.415 | $4^+$ | 4.564 | ${4_1}^+$ | | | | | | |
| 4.441 | $2^+$ | 4.410 | ${2_2}^+$ | | | | | | |
| 4.951 | $2^+$ | | | | | 6.1 | $2^+$ | | |
| 4.974 | $2^-$ | | | 5.628 | ${2_1}^-$ | | | | |
| 5.171 | $5^-$ | | | 4.995 | ${5_1}^-$ | | | | |
| 5.194 | $0^+–3^-$ | 4.702 | ${0_2}^+$ | | | | | | |
| 5.836 | $1^-$ | | | 7.030 | ${1_1}^-$ | | | | |
| 5.856 | $3^-$ | | | 6.199 | ${3_2}^-$ | | | | |
| 5.896 | $4^-$ | | | 6.291 | ${4_1}^-$ | | | | |
| 6.136 | $4^+$ | | | | | 7.4 | $4^+$ | | |
| 6.217 | $5^-$ | | | 6.848 | ${5_2}^-$ | | | | |
| 6.356 | $4^+$ | 6.357 | ${4_2}^+$ | | | | | | |
| 6.632[c)] | | | | | | | | 6.7/5.4 | ${0_1}^+$ |
| 6.730[d)] | $2^+$ | 7.174 | ${2_3}^+$ | | | | | | |
| 6.835 | $4^-$ | | | 6.637 | ${4_2}^-$ | | | | |
| 6.837 | $3^-$ | | | 7.120 | ${3_3}^-$ | | | | |
| 6.867[d)] | $1^+, 2^+$ | 7.099 | ${1_1}^+$ | | | | | | |
| 7.137 | $1^-, 2^+$ | | | | | | | 8.1/7.0 | ${2_1}^+$ |
| 7.140[d)] | $3^+$ | 7.248 | ${3_1}^+$ | | | | | | |
| 7.178[d)] | $1^+, 2^+$ | 8.093 | ${2_4}^+$ | | | | | | |
| 7.247 | $(1–3)^-$ | | | 7.330 | ${2_2}^-$ | | | | |
| 7.259 | $3^-$ | | | 7.909 | ${3_4}^-$ | | | | |
| 7.311[b)] | | | | | | | | /7.6 | ${2_2}^+$ |
| 7.354 | $6^-$ | | | 7.143 | ${6_1}^-$ | | | | |

a) From [13] if not otherwise stated.
b) From [25] corrected for systematic errors of energies.
c) See subsect. 3.3.
d) The assignment of this level to the $0\,\hbar\omega$ configuration is based on its feeding in allowed $\beta$-decay of $^{36}$K [13].
e) Ref. [10].
f) Ref. [11].
g) Read, with 100 keV uncertainty, from fig. 3 of [17].
h) Read, with 100 keV uncertainty, from fig. 3 of [17]/weak-coupling model.

uration. Calculations based on the USD interaction [10] yield unambiguous counterparts, the ${4_1}^+, T = 1$ state at 10310 keV and the ${4_3}^+, T = 0$ state at 8544 keV.

## 4 Assignments of levels to shell-model configurations

The spectrum of high-spin states in table 1 together with the observation [17] of two $J^\pi = 10^+$ states at 11902 and 12748 keV excitation energy reveals a complex structure of $^{36}$Ar which includes $0\,\hbar\omega$, $1\,\hbar\omega$, $2\,\hbar\omega$ and $4\,\hbar\omega$ excitations of the shell model. Weak-coupling calculations along the lines of [26] predict the onset of $3\,\hbar\omega$ excitations at 10 MeV. The proposed structure must be compatible with the spectrum of low-lying levels as it is displayed in table 3 up to the limiting energy of 7.4 MeV where spin-parity assignments to levels start to be less safe. In the following, we discuss both aspects simultaneously, using the theoretical spectra of the different $n\hbar\omega$ configurations obtained from various sources and compiled in tables 1, 3.

$^{36}$Ar is presently the lightest system in the vicinity of the doubly magic nucleus $^{40}$Ca which exhibits the phenomenon of coexisting spherical and deformed shapes. In shell model language it is necessary [8] to consider $4\,\hbar\omega$ excitations in addition to the basic $0\,\hbar\omega$ excitations of equal parity. The deformed shape gives rise to a $K^\pi = 0^+$ rotational band in analogy to previous findings in $^{38}$Ar [6] and $^{40}$Ar [18]. The $J^\pi = 4^+$–$16^+$ members of the band have been identified recently [17] and the $J^\pi = 4^+, 6^+, 8^+$ members at 6136, 7766 and 9929 keV are also present in this work (fig. 3 and table 1). The $J^\pi = 0^+$ and $2^+$ members of the band must be identified, on the basis of the $J(J+1)$ rule of excitation energies, with the 4329 and 4951 keV levels of table 3. In fact, they are not needed for the complete and accurate accounting of the predicted $0\,\hbar\omega$ states. Note in this context that the allowed $\beta$-decay of $^{36}$K [13] depicts the $J = 1$–$3$ states of $0\,\hbar\omega$ origin above 6.2 MeV, where identifications on the basis of excitation energies alone become difficult. Note also that the 9682 keV, $J^\pi = 6^+$ state from the present work accounts for the predicted 9696 keV, $0\,\hbar\omega$ level in table 1. In [17] it was tried to reproduce the rotational states by a shell model calculation in a truncated $4\,\hbar\omega$ space. The band was reproduced with the correct value of the rotational constant but shifted up in energy by roughly 1.3 MeV. The results are included in tables 1, 3. The theoretical partners of the 7766 and 9929 keV levels in table 1 are thus found at 9.1 and 11.1 MeV excitation energy.

The spectrum of negative-parity states which are based on $1\,\hbar\omega$ excitations of the shell model has been calculated in [11] and a brief description of the method is given in the introduction. A one-to-one correspondence can be established (table 3) between the levels with proven negative parity and the prediction. The agreement leads us to assign $J^\pi = 2^+$ to the 7137 keV state which previously had $J^\pi = 1^-, 2^+$ and to infer positive parity for the 6632 and 7311 keV levels. In the realm of high spin and $E_x < 10$ MeV a total of 9 negative-parity $J = 5$–$7$ levels is predicted and the first $J^\pi = 8^-$ should occur at 10783 keV. These states are confronted in table 1 with 6 to 7 levels with $J \le 7$, depending on the assumed parity of the 9186 keV state, plus the 9408 keV level which shows decay to the $J^\pi = 6^-$ yrast state at 7354 keV. The late E.K. Warburton had begun to calculate the $\gamma$-decay of the negative-parity states in $^{36}$Ar. His incomplete results (private communication) show that none of the theoretical $J^\pi = 6^-, 7^-$ levels of table 1 nor the $5_3^-$ state have a sizeable branch to the $6^-$ yrast state. This is a feature of the $J^\pi = 8^-$ yrast state or, less likely, of a higher-lying $J^\pi = 5^-$ or $4^-$ state not yet included in the calculations. The small deficit of experimental negative-parity states with high spin is probably due to the absence of two or three $J^\pi = 5^-$ states. At a suitable excitation energy around 9.5 MeV it is possible that the $\alpha$-decay with $\ell = 5$ and an available energy around 3 MeV dominates the proton decay with $\ell = 3$ and an available energy around 1 MeV. Such levels would be resonances of the $^{32}$S$(\alpha,\gamma)$ reaction but the existing investigations (table 36.18 of [13]) are not sensitive to them because the $\gamma$-decay to the ground and/or first excited state of $^{36}$Ar has been detected only.

At the end of this subsection $2\,\hbar\omega$ excitations of the shell model come into play. We remember the presence of three $E_x < 7.4$ MeV levels in table 3 which are still left without interpretation. A second observation of interest made in [17] is the presence of a $J^\pi = 10^+$ state at 11902 keV, well below the $10^+$ member of the rotational band at 12748 keV. The presence of $2\,\hbar\omega$ excitations accounts for all these facts. The most transparent description is given by the weak-coupling model of Bansal and French [27] in the version of [26]. The model predicts the binding energy of a state with $n$ particles in the $N = 3$ major shell and $m$ holes in the $N = 2$ shell by adopting the binding energies of the particle and, respectively, the hole configuration from experimental states in nuclei with $n$ particles or, respectively, $m$ holes relative to $^{40}$Ca, in the present case $^{42}$Sc and $^{34}$Cl. A schematic particle-hole interaction

$$E_{\text{p-h}} = -n \cdot m \cdot a + b \cdot T_{\text{p}} \cdot T_{\text{h}} + \text{Coulomb corrections} \quad (2)$$

is assumed (monopole interaction) which does not depend on spins but which is strongly dependent on the isospins $T_{\text{p}}$ and $T_{\text{h}}$ of particles and holes and their relative orientation. Standard values are $a = -0.25$ MeV, $b = 2.5$ MeV. The $2\,\hbar\omega$, $T = 0$ states of $^{36}$Ar arise from the isospin coupling schemes $T_{\text{p}} = T_{\text{h}} = 1$ and $T_{\text{p}} = T_{\text{h}} = 0$. The yrast states of the $2\,\hbar\omega$ configuration, which have even spin, arise from the first coupling scheme for $J = 0$–$8$ while the $10^+$ yrast state is due to the second coupling scheme. The low excitation energy of the $10^+$ state is due to the presence of a low-lying $(f_{7/2})^2$ state in $^{42}$Sc with $J^\pi = 7^+$, $T = 0$, $E_x = 616$ keV and of a $(d_{3/2})^{-6}$ or equivalently $(d_{3/2})^2$ state in $^{34}$Cl with $J^\pi = 3^+$, $T = 0$, $E_x = 146$ keV. The $7^+$ state in $^{42}$Sc is the parent of several high-spin states observed in surrounding nuclei by heavy-ion–induced fusion-evaporation reactions [1–5]. A weak-coupling calculation along the lines and with the parameters of [26] places the $10^+$ state at 11.1 MeV close to the experimental value of 11902 keV. The lowest $2\,\hbar\omega$ state with $J^\pi = 0^+$ and $J_{\text{p}} = J_{\text{h}} = 0$, $T_{\text{p}} = T_{\text{h}} = 1$ coupling is predicted at 5.4 MeV. The next two states at 7.0 and 7.6 MeV have $J^\pi = 2^+$ and arise from the recoupling of the particle or, alternatively, the hole angular momenta. The experimental states at 6632, 7137 and 7311 keV in table 3 are obvious counterparts of these three levels. The recoupling of particle spins gives also rise to a $J^\pi = 6^+$ state at 8.6 MeV which could correspond to the experimental state at 9186 keV (table 1). This level was also present in the concurrent work with the $^{24}$Mg$(^{20}$Ne$, 2\alpha)$ reaction [17] which speaks for high spin. The competition between an inherently weak $E1$ decay to the 5171 keV, $J^\pi = 5^-$ yrast state and $E2$ decay to the 4415 keV, $J^\pi = 4^+$ state would not be embarrassing because the $E2$ decay would be forbidden in the case of a pure $2\,\hbar\omega$ configuration of the initial state and a $0\,\hbar\omega$ configuration of the final state. A shell model calculation of $2\,\hbar\omega$ states with a more realistic interaction and a truncated basis space is reported in [17]. The $J^\pi = 0^+$ state is predicted at 6.7 MeV, the $J^\pi = 10^+$

state at 11.2 MeV and the $J^\pi = 6^+$ state at 9.2 MeV confirming the results of the more schematic but transparent weak-coupling predictions.

We conclude that a spectrum of 28 $T = 0$ levels in $^{36}$Ar below 7.4 MeV excitation energy and all observed high-spin states are understood in the frame of the shell model with inclusion of the $0\,\hbar\omega$, $1\,\hbar\omega$, $2\,\hbar\omega$ and $4\,\hbar\omega$ excitations. Below 10 MeV excitation energy all $J \geq 6$ levels seem to be known. The $2\,\hbar\omega$ excitations follow a systematic which has been previously established for $A = 35$–39 nuclei [1–5]. The $4\,\hbar\omega$ excitations can in turn be used to establish systematic for the $A = 36$–40 mass region. This is the topic of the appendix.

## Appendix A. Deformed shapes in the A = 36–40 nuclei

The nuclides $^{40}$Ca, $^{38}$Ar, and $^{36}$Ar have low-lying $K^\pi = 0^+$ rotational bands [7,6,17] with heads at, respectively, 3353, 3377, and 4329 keV excitation energy. They are based on intrinsic states of large prolate deformation with $\varepsilon$-values [28] ranging from 0.3 in $^{38}$Ar to 0.4 in $^{36}$Ar. The Fermi boarder in the Nilsson [28] level scheme of $^{36}$Ar occurs, for $\varepsilon > 0.32$, between the $\Omega^\pi = 1/2^-$ [330] and the $\Omega^\pi = 1/2^+$ [200] orbits. The fourfold occupation of the negative-parity orbit implies that we are dealing with a $4\,\hbar\omega$ excitation. The $K^\pi = 0^+$ band in $^{38}$Ar is generated by adding to the deformed $^{36}$Ar core a pair of $\Omega^\pi = 1/2^+$ nucleons, coupled to $K'$, $T' = 0, 1$, while the $^{40}$Ca band is generated by saturating the orbit. By the same token $K^\pi = 1/2^+$ bands must exist in the mirror pairs $^{37}$Ar-$^{37}$K and $^{39}$K-$^{39}$Ca. The doubly odd nucleus $^{38}$K must show a $K^\pi = 1^+$, $T = 0$ band and a $K^\pi = 0^+$, $T = 0$ band with members of odd spin in addition to the $K^\pi = 0^+$, $T = 1$ band already known from $^{38}$Ar. All of the predicted states constitute $4\,\hbar\omega$ excitations and their identification rests on the control of the $0\,\hbar\omega$ and $2\,\hbar\omega$ excitations. The following discussion is based on the compilation of experimental data in [13].

The $J^\pi, T = 1/2^+, 1/2$ levels of $0\,\hbar\omega$ origin in $A = 37$, 39 are predictable with 200 keV accuracy [10] and completely known ($E_x = 2523/2469$ in $^{39}$K/$^{39}$Ca, $E_x = 1371/1410$; 4509/(4318) keV in $^{37}$K/$^{37}$Ar and 5450 keV in $^{37}$K). There is consensus between weak coupling and more elaborate shell model calculations [29] that the first $1/2^+$ state of $2\,\hbar\omega$ origin occurs between 1.2 and 1.5 MeV above the lowest-lying level of the same configuration, which has $J^\pi = 3/2^+$ and excitation energy of, respectively, 3939 keV in $^{39}$K and 3937 keV in $^{37}$Ar. A $J^\pi = 1/2^+$ state is in fact established at 5123 keV in $^{37}$K and the spectrum of $^{39}$K provides a low-spin state at 5173 keV without further candidates below 6 MeV. What is left as prospective $K^\pi = 1/2^+$ bandhead in $A = 37$ or 39 is the 4095 keV, $J^\pi = 1/2^+$ state in $^{39}$K and the 3980 keV level in $^{37}$Ar which has a most likely assignment of $J^\pi = 1/2^+$ [2]. The identification made in $^{37}$Ar can be checked for plausibility. Brink and Kerman [30] have established an energetical relation between rotational bands which arise from the successive filling of the same Nilsson orbit. Applied to the present case it reads $^{40}\mathrm{Ca} - {}^{36}\mathrm{Ar} = {}^{39}\mathrm{Ca} + {}^{39}\mathrm{K} - {}^{37}\mathrm{K} - {}^{37}\mathrm{Ar}$, where the symbols stand for binding energies of bandheads in the respective nuclide. By assuming equal excitation energies of mirror analogue states in $A = 37$, 39 we deduce an excitation energy of 4220 keV for the $J^\pi = 1/2^+$ bandhead in $A = 37$, very close to the experimental value of 3980 keV.

Coming to $^{38}$K we notice first that levels at 3702 and 4214 keV are readily identified, on the basis of Coulomb-energy systematic, as first members of the $K^\pi = 0^+, T = 1$ band already known from $^{38}$Ar [6]. There is consensus between shell model calculations [10,29] and weak-coupling calculations that the $T = 0$ spectrum of $^{38}$K contains four $J^\pi = 1^+$ states at most, if $0\,\hbar\omega$ and $2\,\hbar\omega$ excitations are considered only. Experimentally we observe the fourth and fifth level at 3857 and 3978 keV already and more candidates at higher energy, starting with the 4175 keV, $J^\pi = 1^+, 2^+$ level. At least one of the $J^\pi = 1^+$ bandheads is thus present.

To conclude with we have identified heads of rotational bands in all *s-d* shell nuclei between $^{36}$Ar and $^{40}$Ca at remarkably uniform excitation energies between 3.3 and 4.3 MeV. They constitute $4\,\hbar\omega$ excitations which compete successfully with $2\,\hbar\omega$ excitations.

Last but not least, we complete the systematic of deformed states in the Ar isotopes with large neutron excess. The nuclide $^{40}$Ar shows a $K^\pi = 0^+$ rotational band [18] which can be generated from the $^{38}$Ar deformed state by adding a $K', T' = 0, 1$ pair of nucleons in either the sphericity driving $\Omega^\pi = 3/2^+$ [202] or the deformation driving $\Omega^\pi = 3/2^-$ [321] orbit. The increase of the intrinsic quadrupole moment from roughly 850 mb in $^{38}$Ar [6] to 1300 mb in $^{40}$Ar [18] points at the $\Omega^\pi = 3/2^-$ level which dives below the $\Omega^\pi = 3/2^+$ level for $\varepsilon > 0.4$. Consequently a $K^\pi = 3/2^-$ band is expected in $^{39}$Ar. The spectrum of negative-parity states is well under control by shell model calculations in a $0\,\hbar\omega$ space [11]. They fail, however, to predict the 2342 keV, $J^\pi = 3/2^-$ state. According to our interpretation it must constitute a $4\,\hbar\omega$ excitation rather than a $2\,\hbar\omega$ excitation. The same holds for the rotational states of $^{40}$Ar.

## References


1. E.K. Warburton, J.W. Olness, A.R. Poletti, J.J. Kolata, Phys. Rev. C **14**, 996 (1976).
2. P.J. Nolan, L.L. Gadeken, A.J. Brown, P.A. Butler, L.L. Green, C.J. Lister, A.N. James, J.D. McArthur, J.F. Sharpey-Schafer, D.A. Viggars, J. Phys. G **1**, 35 (1975).
3. E.K. Warburton, J.W. Olness, J.J. Kolata, A.R. Poletti, Phys. Rev. C **13**, 1762 (1976).
4. C.J. Van der Poel, G.A.P. Engelbertink, H.F.R. Arciszewski, P.C.N. Crouzen, J.W. de Vries, E.A.J.M. Offerman, E.J. Evers, Nucl. Phys. A **394**, 501 (1983).
5. H.H. Eggenhuisen, L.P. Ekström, G.A.P. Engelbertink, H.J.M. Aarts, Nucl. Phys. A **305**, 245 (1978).
6. P. Betz, H. Röpke, F. Glatz, G. Hammel, V. Glattes, W. Brendler, Z. Phys. **271**, 195 (1974).

7. A.M. Nathan, J.J. Kolata, Phys. Rev. C **14**, 171 (1976).
8. W.J. Gerace, A.M. Green, Nucl. Phys. A **93**, 110 (1967).
9. Th. Kern, P. Betz, E. Bitterwolf, F. Glatz, H. Röpke, Z. Phys. A **294**, 51 (1980).
10. B.H. Wildenthal, in *Progress in Particle and Nuclear Physics*, edited by D.H. Wilkinson (Plenum Press, New York, 1984) p. 1 and private communication.
11. E.K. Warburton, J.A. Becker, D.J. Millener, B.A. Brown, Brookhaven National Laboratory Report, 40890 (1987) unpublished.
12. J.B. McGrory, Phys. Rev. C **8**, 693 (1973).
13. P.M. Endt, Nucl. Phys. A **521**, 1 (1990); **633**, 1 (1998).
14. J. Brenneisen, B. Erhardt, F. Glatz, Th. Kern, R. Ott, H. Röpke, J. Schmälzlin, P. Siedle, B.H. Wildenthal, Z. Phys. A **357**, 157 (1997).
15. F. Glatz, J. Siefert, P. Betz, E. Bitterwolf, A. Burkard, F. Heidinger, Th. Kern, R. Lehmann, S. Norbert, H. Röpke, Z. Phys. A **303**, 239 (1981).
16. F. Glatz, M. Lickert, A. Burkard, Th. Kern, R. Lehmann, S. Norbert, H. Röpke, J. Siefert, Z. Phys. A **324**, 173 (1986).
17. C.E. Svensson *et al.*, Phys. Rev. Lett. **85**, 2693 (2000); Phys. Rev. C **63**, 061301 (R) (2001).
18. E. Bitterwolf, A. Burkard, P. Betz., F. Glatz, F. Heidinger, Th. Kern, R. Lehmann, S. Norbert, H. Röpke, C. Schneider, J. Siefert, Z. Phys. A **313**, 123 (1983).
19. P. Betz, G. Braun, G. Hammel, J. Urban, Nucl. Instrum. Methods **119**, 199 (1974).
20. P.M. Endt, At. Data Nucl. Data Tables **55**, 171 (1993).
21. P.M. Johnson, M.A. Meyer, D. Reitmann, Nucl. Phys. A **218**, 333 (1974).
22. J. Brenneisen, D. Grathwohl, M. Lickert, R. Ott, H. Röpke, J. Schmälzlin, P. Siedle, B.H. Wildenthal, Z. Phys. A **352**, 279 (1995).
23. H.J. Rose, D.M. Brink, Rev. Mod. Phys. **39**, 306 (1967).
24. P.J. Twin in *The Electromagnetic Interaction in Nuclear Spectroscopy*, edited by W.D. Hamilton (North Holland, Amsterdam, 1975) p. 701.
25. R.G. Allas, L. Meyer-Schützmeister, D. von Ehrenstein, Nucl. Phys. **61**, 289 (1965).
26. J.J. Kolata, J.W. Olness, E.K. Warburton, A.R. Poletti, Phys. Rev. C **13**, 1944 (1976).
27. R. Bansal, J. French, Phys. Lett. **11**, 145 (1964).
28. S.G. Nilsson, Mat.-Fys. Medd. K. Dan. Vidensk. Selsk. **29**, no. 16 (1955).
29. H. Hasper, Phys. Rev. C **19**, 1482 (1979).
30. D.M. Brink, A.K. Kerman, Nucl. Phys. **12**, 314 (1959).